

# Time Synchronised Distributed Acoustic Sensing of Partial Discharge at the Oil-Pressboard Interface

Laurie Kirkcaldy<sup>id</sup>, Gareth Lees<sup>id</sup>, Rosalie Rogers<sup>id</sup>, Paul Lewin<sup>id</sup>

**Abstract**—Distributed Acoustic Sensing (DAS) is a well-established technology used across a variety of industries. Due to its inherently low sample rates at detection ranges of a couple hundred metres or more, at face value, it appears ineffective for Partial Discharge (PD) detection and therefore has not been previously used. However, in this publication, we show that aliasing effects due to the DAS sampling methods successfully down-sample the higher frequency acoustic emissions and can provide detection of PD above 120 pC under treeing discharge across an oil-pressboard interface. This is supported with comparisons between DAS, high-sample rate acoustic sensors, as well as industry standard electrical measurements. Synchronization between the different measurement systems is achieved allowing for sample-to-sample comparison as well as a more statistical approach. We additionally show Phase Resolved Partial Discharge (PRPD) analysis can be applied to the DAS results with an additional voltage zero-crossing synchronisation signal, with a clear resemblance to electrical methods.

**Index Terms**—Partial discharge (PD), distributed acoustic sensing (DAS), void discharge, treeing, high voltage, acoustics, acoustic emission.

## I. INTRODUCTION

Partial discharge is known to be a prominent indicator, and contributing factor, of insulation failure within high voltage equipment [1]. Many methods for detection are used today including electrical, acoustic, radio and chemical [2], [3]. However, none of these methods are able to provide long detection ranges or exact localisation of Partial Discharge (PD) events without the use of multiple costly discrete sensors [3], [4]. Fibre systems which have these long ranges of kilometres or more have been previously used for PD detection using Bragg Gratings [5] or single-ended sensors [6], typically using an interferometer system for measurement. However, this does not provide a continuous detection array and requires these sense regions to be specifically placed where detection is required.

Distributed Acoustic Sensing (DAS) provides an acoustic based method of detection, whilst also providing exact location and continuous detection distances up to many kilometres. DAS does not require a specific sensor element, it instead utilises cheap, standard single mode telecommunication fibres that may already be embedded in HV plant. As the sensing

element is simply a glass fibre, it is also inherently immune to electrical or magnetic noise.

DAS, however, does have a limited sample rate, primarily due to the round-trip time of light down the fibre. Because of the sampling techniques of DAS, we demonstrate that higher frequencies like those emitted from Acoustic Emissions (AE) of PD are still able to be successfully detected, despite when the sample rate is as low as 20 kHz, achieving 5.1 km of usable detection range. The use of DAS also allows for mechanical damage detection [7] as well as fault detection [8], [9] utilising the same strain data.

DAS works on the same principles of other acoustic sensors by looking for minute vibrations and therefore strain caused by AE originating from PDs, but instead has a continuous sensing array provided by the fibre optic itself. Therefore, multiple separated sources of PD can be detected across the length of measurement simultaneously. Following on from initial proof-of-concept work with DAS as a detection method [10], this paper displays results and individual event comparisons of electrical, high bandwidth acoustic and DAS systems of treeing discharge at the oil-pressboard interface primarily used in transformers.

## II. DISTRIBUTED ACOUSTIC SENSING

DAS measures the strain along a fibre optic using Rayleigh backscatter using the well understood technique of Coherent Optical Time Domain Reflectometry (c-OTDR) [11]. A highly coherent laser is pulsed launching light pulses down a single-mode fibre optic cable. Rayleigh backscatter occurs within the fibre, causing some reflection of the launched pulse back-towards the source. The backscatter is then measured by constructing an interferometer with the laser and the returning light. By measuring how this backscatter changes over successive interrogations of the fibre, strain on the fibre over time can be recorded [12], and therefore an acoustic signal is extracted. Distance information of a vibration event can be determined by comparing the time of launch to detected reflections, given the known speed of light down the fibre.

The strain changes measured for each channel or “distance bin” of measurement are not a point measurement but are integrated over a distance known as the spatial resolution or gauge length. Given the phase data from the backscatter, gauge lengths can be overlapped on top of each other for the same fibre interrogation by a distance known as the spatial sampling

distance or channel spacing, increasing the resultant distance resolution. The gauge length is required to be long enough to obtain an optimal Signal to Noise Ratio (SNR) [13] whereas the spatial sampling distance only need to be longer than the duration of the laser pulse [14]. The DAS channel spacing used in these experiments was 1.27 m, and the gauge length was 5 m. This means for an acoustic event, the detected energy will be spread across a gauge length, but the closest channel will have the highest peak energy thereby giving a more-accurate location than the gauge length.

The sample rate of a DAS system without additional methods [15] is the round-trip time of light to the end of the fibre. Therefore, the distance limit,  $D$ , of a required sample rate,  $f$ , is given by  $D = \frac{v}{2f}$ , where  $v$  is the speed of light within the fibre and can be determined from the refractive index:  $v = \frac{c}{n}$ .  $n \approx 1.47$  for a Single-Mode (SM) glass fibre. For example, at a rate of 100 kHz the maximum distance achievable is 1.02 km; at the sample rate used in these experiments of 20 kHz, the maximum distance is 5.10 km.

### A. Undersampling

Whilst the DAS' sample rate is only 20 kHz, it is possible for the system to detect the presence of higher frequency acoustic signals. This occurs as, due to the interrogation of the fibre by a short laser pulse, the sample window is on the order of 10 ns [14]. Therefore, if a DAS sample window occurs during an AE signal of higher frequency, the recorded optical phase will approximately correlate to the envelope of the high frequency signal, given the window did not occur at a zero-crossing. The high frequency information of the original signal will be lost, but identification of the event occurring will be recorded [10]. This phenomenon is described as an aliasing or undersampling effect and is typically unwanted by many low-sample rate systems [16].

Additionally, due to this distortion of the originating signal, many de-noising techniques such as bandpass filtering or discrete wavelet transforms applied to other PD measurement methods are unsuitable in this application.

## III. EXPERIMENT SETUP AND PROCEDURE

A 5 mm thick 100x100 mm section of Weidmann Transformerboard TIV pressboard was prepared to 6% moisture content by weight and placed in an oil bath to reduce further moisture absorption. The thickness of pressboard was selected to ensure that surface discharge was the dominant degradation mechanism and the board would not mechanically fail during the experiment. The setup and procedure was designed to replicate experiments from [17] and [18], reproducing types of discharge observed within power transformers and other devices containing similar pressboard insulation. The moisture content drives how fast the degradation of the pressboard progresses and therefore is not critical in this experiment other than limiting the experiment time-frame. A needle was placed at a shallow angle to the pressboard and connected to a variable high voltage source. An earthed copper bar was perpendicularly attached 30 mm from the tip of the needle as shown in Fig. 1. This needle-bar configuration ensures that

built-up charges around the needle tip are spread across the pressboard surface, rather than penetrating into the underlying bulk material [19]; therefore, preferring discharges across the surface leading to tracking discharge. The voltage was increased to the inception point of PD and allowed to progress through initial corona and surface discharge up to treeing as described in [18]. Electrical measurement was continued throughout as to monitor discharge progression. DAS, and AE were sampled at various points during the progression as to provide a variety of sampled discharge sizes.

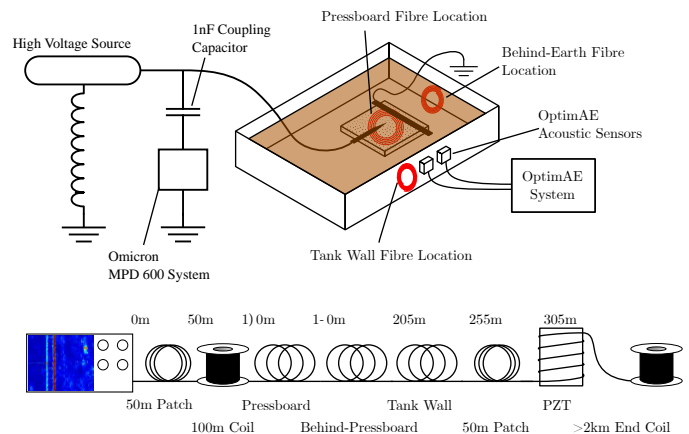


Fig. 1. Diagram of the pressboard experiment detailing fibre positions and electrical connections. The 3 fibre positions shown are: mechanically attached underneath the pressboard, suspended in oil near the tank wall and OptimaE sensors, and behind the grounding bar.

### A. Electrical Partial Discharge Measurement

An industry standard Omicron MPD600 system was utilised for recording electrical events, as well as resolving the PD patterns for use of condition monitoring under IEC60270. This was also used as a measurement of the applied voltage and for analysing inception points for the PD. The maximum measured noise level up to 30 kV of the HV setup without the needle present was 12 pC, and as most discharges studied in this experiment are above 100 pC, a threshold level of 20 pC was chosen below which events were discarded. This method was chosen over a direct recording into, for example, a digital oscilloscope due to the duration of data captures required for comparison to acoustic methods.

### B. Acoustic Measurement

For the measurement of acoustic signals at a high sample rate and sensitivity, an Optics11 OptimaE system was used. This was chosen over other methods as the optical measurements ensure immunity to electric and magnetic fields, and also provided a better comparison of distributed optical methods versus discrete. The OptimaE system consists of a central measurement unit and multiple sensor heads. Each measurement head is sampled separately to allow for multiple channels of independent measurement. Each channel acts as an optical interferometer, with a Fabry-Pérot cavity [20] at the sensing end. This allows for extremely small disturbances to be measured, down to below single nanometres of movement

of the sensor head, at sample rates of one mega-sample per second (1 MS/s). A total of 3 sensors were utilised, 2 for measurement of PD, and one extra sensor for synchronisation.

### C. DAS Fibre Layout

The DAS fibre layout consisted of a 100 m launch coil internal to the DAS unit, 50 m of patch cable to bring the fibre to the experimental area, an acoustically decoupled 100 m coil to reduce the background noise of the experimental section, and then alternating sections of measurement and spacing fibre. 10 m of spacing fibre were placed between measurement sections to ensure that different areas did not influence each other.

The first measurement sections bonded to the pressboard with cyanoacrylate consisted of: 5 m, 3 m and a single pass of fibre. In addition, 5 m, 3 m, 1 m and a single pass of fibre were submerged in the oil tank against the wall; next to which the high-sample rate sensors were held in place on the outside of the tank with a clamp stand and mated using ultrasonic coupling gel. This allowed for comparison event amplitudes from different fibre lengths in contact with, and separated in oil. An additional 5 m of fibre was placed behind the pressboard, still submerged in oil, but without direct line of sight of the top side of the discharge area to investigate acoustic shading effects from the pressboard compared with the other sensing areas.

The fibre path then consisted of another 50 m patch fibre into a Piezo-Electric Transducer (PZT) allowing injection of custom pulses into the DAS data at its location. Finally, a long coil (greater than 2 km in length) was used as a receive coil to ensure end reflections did not affect any measurement sections. All fibres used were SMF-28 and interrogated simultaneously with the DAS system. The coils of fibre used in measurement sections were used to increase the sensitivity at these specific points as well as provide a comparison for the different lengths of bundled fibre. An overview of the fibre connections can be found in Fig. 1.

### D. Synchronisation

Synchronising the different measurement systems was achieved through manually triggered synchronisation pulses, rather than timestamp-alignment as the Omicron system does not support absolute timestamps of data. The synchronisation pulses were injected into the PD input of the electrical system and split into a pulse generator to form correctly shaped driving signals to the PZT. This also provided synchronisation to the high sample rate acoustic sensors through a mounted sensing element on the PZT.

After capture of data, these synchronisation pulses are scanned for and used to generate an offset per data capture system. These time offsets can then be subtracted lining up an absolute zero point across all data. Without this custom synchronisation, the widely different sample rates and data formats would not be able to be compared at the individual PD event level. The synchronisation achieved between systems is  $<1$  ms and obtains a drift of less than  $15 \text{ ms h}^{-1}$ . This is mostly limited by the PC-based timing jitter of the Omicron

system and therefore data captures are kept under 2 minutes with synchronisation completed before each data capture to reduce the effects of this drift.

## IV. RESULTS

Partial Discharge was initiated at the needle tip causing initial surface discharges at an inception voltage of 19 kV. The pressboard was then allowed to progress through to drying stages and finally treeing under the same applied voltage after a period of an hour. Indication of the progression was monitored through the electrical system as well as observable changes on the pressboard surface: black tracking and evidence of drying seen as lighter regions of the pressboard, shown in Fig. 2. The average PD amplitude decreased to 600 pC after these observations, with peaks of 2.2 nC and rates of 120 PDs per second.

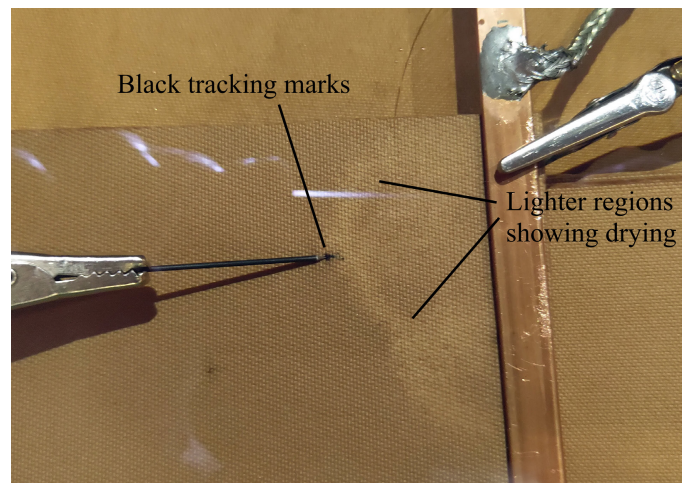
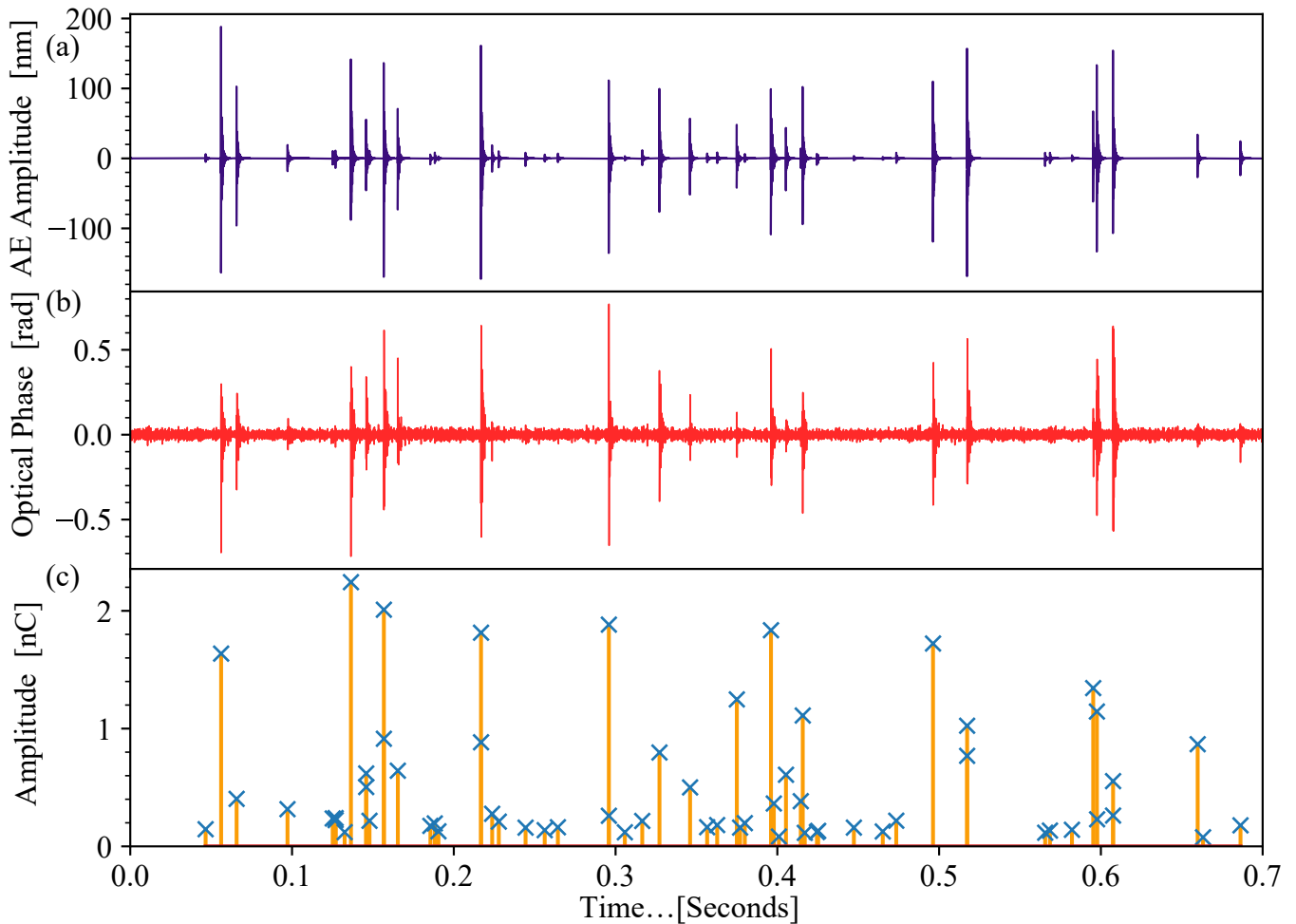
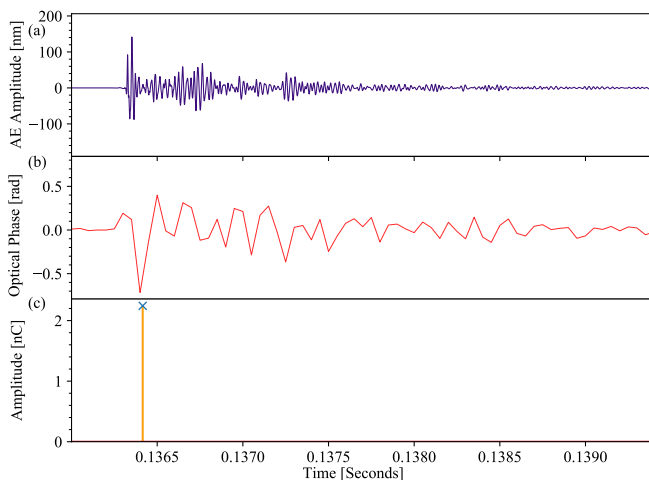


Fig. 2. Picture of the needle-bar setup on the pressboard after 1 hour of applied voltage. Black tracking marks are seen emanating from the needle tip and lighter branching regions showing drying of the pressboard.

Fig. 3 shows the high sample rate acoustic sensors, DAS output of the 3 m coil of fibre suspended in the oil near the tank wall and the reference electrical system synchronised together. The 3 m measurement section was used as it contains the best signal to noise ratio as detailed in Section IV-B. Spikes from PD events can be seen clearly to line up in all systems. A rough correlation can be observed between the amplitude of the PD and the size of the AE in the high sample rate system and DAS. Many events in this period of discharge are significantly lower in amplitude for both acoustic methods compared to the high levels seen during surface discharge [10]. This is mostly due to the position of the discharge, as well as the original AE size difference. During surface discharge the arcs form across the surface, easily transferring acoustic energy into the surrounding oil. However, for treeing discharge, most of the acoustic energy is contained in the bulk of the material. Pressboard due to its composite composition is an excellent damping material, absorbing acoustic energy and therefore attenuating the resultant acoustic amplitude.



**Fig. 3.** Amplitude of Acoustic Emissions in purple, as measured by the acoustic sensor. Measured in displacement of sensor element. (b) Optical phase output of the DAS system in red, corresponding to the 5 m coil of fibre suspended in oil next to the OptimAE sensor. (c) Absolute amplitude of PD events in amber, as measured by the electrical system. As the events recorded by the electrical system are not continuous, the crosses indicate partial discharge events with the vertical lines added for better clarity.



**Fig. 4.** Zoomed in detail of a PD event from Figure 3. (a) Amplitude of Acoustic Emissions in purple, as measured by the Optics11 OptimAE sensor. Measured in displacement of sensor element. (b) Optical phase output of the DAS system in red, corresponding to the 5 m coil of fibre suspended in oil next to the OptimAE sensor. (c) Absolute amplitude of PD events in amber, as measured by the Omicron MPD600 system.

Looking at a single event from Fig. 3 at 136.4 ms in more detail (Fig. 4), the AE impulse followed by ringing is seen by both acoustic systems, albeit with distortion in the DAS due to undersampling. The damped ringing after the initial impulse is from reflections off the geometry of the surrounding materials. The lower sample rate DAS maintains following the envelope of the source AE and picks up the initial higher amplitude spike.

In this initial data capture, PDs under 500 pC in amplitude are rarely seen in the DAS data, and corresponding peaks in the AE sensors are orders of magnitude smaller. After 30 minutes of further treeing discharge, the larger PDs of over 500 pC stop occurring as the surrounding area from the needle dries out and tracking at the branch tips becomes the primary discharge. During the following discharge, lower amplitude events that were not previously seen in the DAS increase in number. Fig. 5 shows these events with similar features to the previous PDs.

The peak amplitude of these events in the DAS data is much closer to the noise floor due to the AE being smaller in amplitude as seen by the discrete sensors, with the smallest repeatable event with a noticeable change in strain of a PD

amplitude of approximately 120 pC. These peaks dropping below the noise floor, however, do not constitute the minimum sensitivity. For example, at 70 ms and 150 ms in Fig. 5 PD events of 200 pC and 300 pC both register the same peak DAS amplitude of 0.9 rad. This is because the sampling window of the DAS misses the initial spike and only picks up later ringing. As the size of the AE is quite small, only the first few microseconds of the impulse are large enough to produce a measurable DAS output, and therefore DAS can detect these smaller events but only if the sampling window happens to line up with the initial spike. This demonstrates an important undersampling effect resulting in the DAS amplitude not always representing the true AE size, and therefore the origin PD amplitude. By taking multiple events into account rather than focussing on individual events, a trend can be established from the peaks of DAS data.

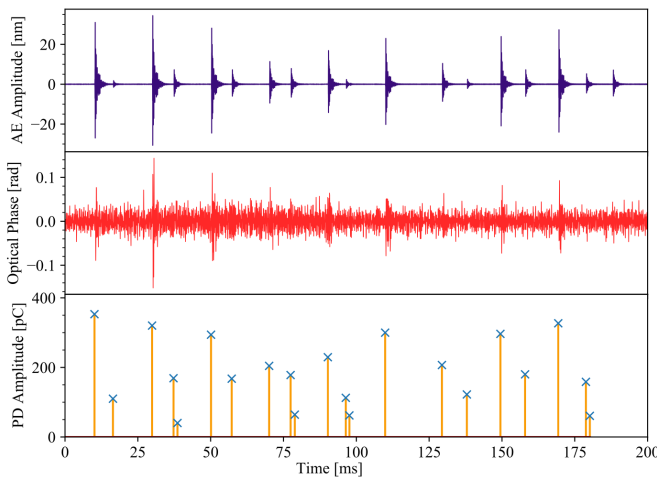


Fig. 5. Amplitude of PDs from the acoustic sensors, DAS and electrical systems during later treeing discharge, time synchronized. Peak PD amplitudes of 380 pC and rates of 95 PDs/s.

### A. PRPD Analysis of DAS

By triggering the PZT used for synchronisation from a zero-crossing detector referenced to the high voltage source during data capture, the voltage phase can be determined for each spike seen in the DAS. This turns the DAS data from a continuous-time optical phase data capture into a list of PD events with associated time and voltage phase. By plotting these events in a scatter plot, the DAS-detected PD events can have PRPD analysis applied.

Fig. 6 shows the PRPD plot generated from the DAS data for a 100 second data capture of pressboard discharge. In comparison, an Omicron generated plot of the same measurement period generated from the electrical measurement is shown on the right. Both plots clearly show similar patterns with increased intensity of lower amplitude discharge in the positive half-cycle in addition to higher peak values, and less amplitude of discharge on the negative cycle. PRPD analysis also allows for some separation of noise and discharge events: noise will appear with no correlation across the plot, whereas discharge events tend to occur in specific patterns relative to the AC waveform.

### B. Comparison of Sensing Locations

As previously mentioned, data was also recorded from different lengths of test fibre in contact with the pressboard and submerged in the oil tank to investigate the effect of fibre shorter than the gauge length on the resultant event amplitude. Fig. 7 shows PD events from all fibre sections during treeing discharge. All 3 positions of fibre (in contact with, behind pressboard and by tank wall) detect the incident AE, with the highest amplitudes observed in the fibre by the tank wall. This is again due to the AE being absorbed within the pressboard, and therefore the fibres mechanically mounted on the bottom of the pressboard experiencing less strain change.

Regions consisting of less than 3 m of sense fibre have a significantly reduced maximum amplitude compared to other

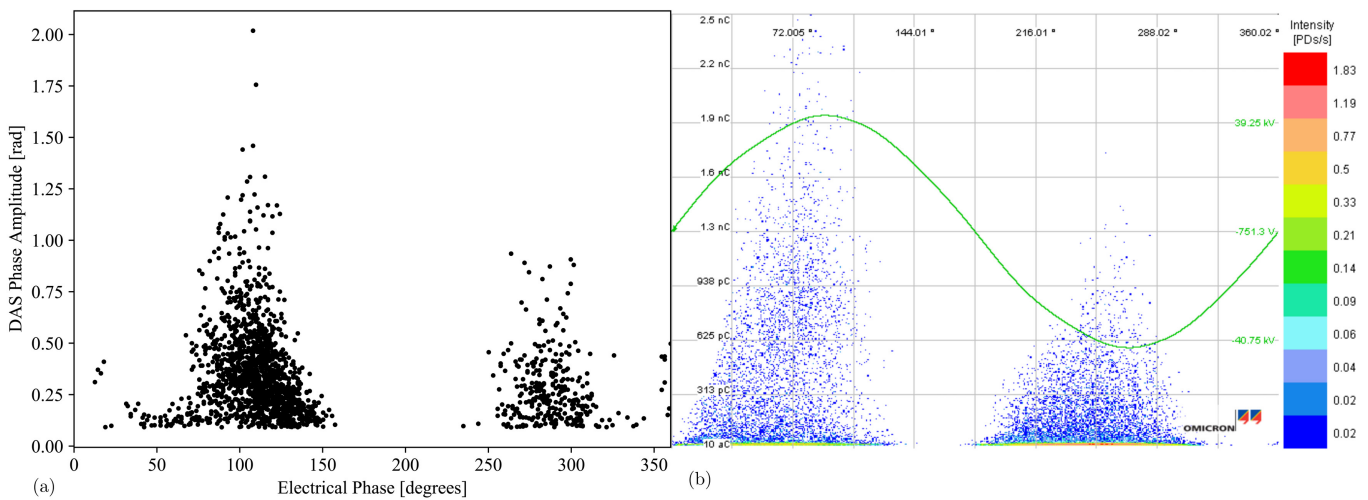


Fig. 6. PRPD plots of the DAS (a) and electrical (b) systems. A strong correlation between the two graphs can be seen with higher amplitude events occurring in the positive half-cycle. The DAS shows fewer detected events in the negative half-cycle, possibly due to reduced PD amplitude resulting in more events below the noise floor.

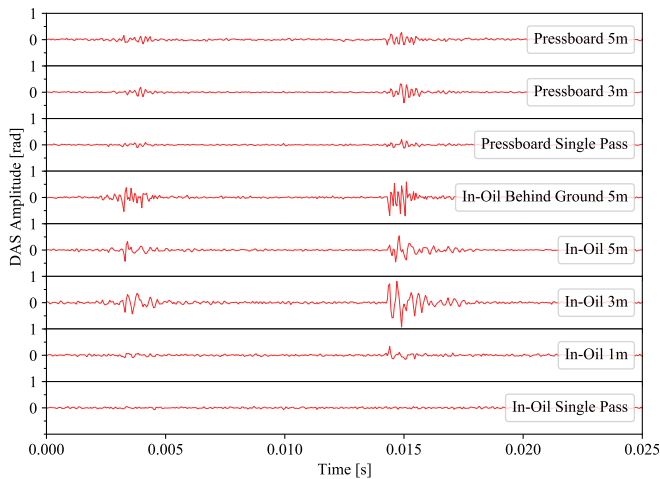


Fig. 7. Comparison of different DAS amplitude at different fibre positions and lengths of sense fibre. 2 Partial Discharge events seen. A single pass refers to a length of around 15 cm, enough for the fibre to enter and exit the oil at the specified position.

locations, with the 3 m sections appearing to experience the highest strain change. The significant reduction in amplitude appears to occur at the transition between 3 m and below, at approximately half the gauge length (2.5 m). The 5 m sections, despite having the greatest coiled length covering exactly a gauge length, shows a lower amplitude than the 3 m. This is either due to the larger coil of fibre creating a larger acoustic impedance change, or cancellation effects from the averaging across the gauge length.

The position of fibre behind the pressboard was not in line of sight to the top surface of the pressboard. Therefore as a significant strain change is observed, this demonstrates AE can still be detected from the diffraction and reverberation off surrounding materials without a clear line of sight, given no absorptive materials are in the wave path from source to sensing fibre.

## V. CONCLUSION

This research has demonstrated that partial discharge detection can be achieved using DAS down to PD amplitudes of 120 pC during treeing discharge. Due to the fibre interrogation method, locations of these events are inherently known. The unique undersampling processes with DAS are shown to allow low sample rate DAS systems to be able to detect the high frequency AE produced by PDs. Given the current requirement for a repeated segment of fibre, at least half the gauge length, and the range of detectable PD, the authors believe this DAS method is currently best suited for application of detection of PDs within high voltage transformers. As no discrete sensors are required, continuous fibres could easily be wound within windings, or utilise existing temperature sensing fibres, providing useful detection and pinpointing within the transformer of partial discharge events despite tank reverberations due to the continuous fibre optic providing proximity to possible discharge sites. Analysis techniques such as PRPD can also be utilised given a zero-crossing synchronisation signal is also recorded alongside the optical data.

## ACKNOWLEDGMENTS

The support from APSensing and the lab technicians at the Tony Davies High Voltage Laboratory is greatly appreciated, along with thanks given to Optics11 for the generous loan of an interferometer based acoustic sensing solution: OptimAE.

## REFERENCES

- [1] S. A. Boggs, "Partial Discharge: Overview and Signal Generation," *IEEE Electrical Insulation Magazine*, vol. 6, no. 4, pp. 33–39, 1990. [Online]. Available: <https://doi.org/10.1109/57.63057>
- [2] Y. Tian, P. L. Lewin, J. S. Wilkinson, S. J. Sutton, and S. G. Swingler, "Continuous on-line monitoring of partial discharges in high voltage cables," in *Conference Record of IEEE International Symposium on Electrical Insulation*, 2004, pp. 454–457. [Online]. Available: <https://doi.org/10.1109/elinsl.2004.1380640>
- [3] M. M. Yaacob, M. A. Alsaedi, J. R. Rashed, A. M. Dakhil, and S. F. Atyah, "Review on partial discharge detection techniques related to high voltage power equipment using different sensors," *Photonic Sensors*, vol. 4, no. 4, pp. 325–337, dec 2014. [Online]. Available: <https://doi.org/10.1007/s13320-014-0146-7>
- [4] N. Saravanakumar and K. Sathiyasekar, "Circular Array of Ultrasonic Sensor based DOA estimation: Location of multiple Partial Discharge in Transformer oil," *Journal of Electromagnetic Waves and Applications*, vol. 32, no. 12, pp. 1569–1585, aug 2018. [Online]. Available: <https://doi.org/10.1080/09205071.2018.1456365>
- [5] M. R. Hussain, S. S. Refaat, and H. Abu-Rub, "Overview and Partial Discharge Analysis of Power Transformers: A Literature Review," pp. 64 587–64 605, 2021. [Online]. Available: <https://doi.org/10.1109/ACCESS.2021.3075288>
- [6] J. Deng, H. Xiao, W. Huo, M. Luo, R. May, A. Wang, and Y. Liu, "Optical fiber sensor-based detection of partial discharges in power transformers," *Optics and Laser Technology*, vol. 33, no. 5, pp. 305–311, jul 2001. [Online]. Available: [https://doi.org/10.1016/S0030-3992\(01\)00022-6](https://doi.org/10.1016/S0030-3992(01)00022-6)
- [7] K. Hicke and K. Krebber, "Towards efficient real-time submarine power cable monitoring using distributed fibre optic acoustic sensors," in *25th International Conference on Optical Fiber Sensors*, vol. 10323. SPIE, apr 2017, p. 1032390. [Online]. Available: <https://doi.org/10.1117/12.2267474>
- [8] G. Ma, W. Qin, C. Shi, H. Zhou, Y. Li, and C. Li, "Electrical Discharge Localization for Gas Insulated Line Based on Distributed Acoustic Sensing," in *Lecture Notes in Electrical Engineering*. Springer, 2020, vol. 598 LNEE, pp. 606–614. [Online]. Available: [https://doi.org/10.1007/978-3-030-31676-1\\_{\\_}57](https://doi.org/10.1007/978-3-030-31676-1_{_}57)
- [9] S. Cherukupalli and G. J. Anders, "Use of Distributed Sensing for Strain Measurement and Acoustic Monitoring in Power Cables," in *Distributed Fiber Sensing and Dynamic Rating of Power Cables*, 1st ed. Wiley, sep 2019, ch. 11, pp. 185–209. [Online]. Available: <https://doi.org/10.1002/9781119487739.ch11>
- [10] L. Kirkcaldy, P. Lewin, G. Lees, and R. Rogers, "Partial Discharge Detection Using Distributed Acoustic Sensing at the Oil-Pressboard Interface," in *IEEE Sensors Applications Symposium*, Virtual, 2021.
- [11] A. Masoudi and T. P. Newson, "Contributed Review: Distributed optical fibre dynamic strain sensing," *Review of Scientific Instruments*, vol. 87, no. 1, p. 011501, jan 2016. [Online]. Available: <https://doi.org/10.1063/1.4939482>
- [12] A. Masoudi, M. Belal, and T. P. Newson, "A distributed optical fibre dynamic strain sensor based on phase-OTDR," *Measurement Science and Technology*, vol. 24, no. 8, p. 085204, aug 2013. [Online]. Available: <https://doi.org/10.1088/0957-0233/24/8/085204>
- [13] H. Gabai and A. Eyal, "On the sensitivity of distributed acoustic sensing," *Optics Letters*, vol. 41, no. 24, p. 5648, dec 2016. [Online]. Available: <https://doi.org/10.1364/ol.41.005648>
- [14] A. Mateeva, J. Lopez, H. Potters, J. Mestayer, B. Cox, D. Kiyashchenko, P. Wills, S. Grandi, K. Hornman, B. Kuvshinov, W. Berlang, Z. Yang, and R. Detomo, "Distributed acoustic sensing for reservoir monitoring with vertical seismic profiling," *Geophysical Prospecting*, vol. 62, no. 4, pp. 679–692, jul 2014. [Online]. Available: <https://doi.org/10.1111/1365-2478.12116>
- [15] G. Yang, X. Fan, Q. Liu, and Z. He, "Increasing the frequency response of direct-detection phase-sensitive OTDR by using frequency division multiplexing," in *25th International Conference on Optical Fiber Sensors*, Y. Chung, W. Jin, B. Lee, J. Canning, K. Nakamura, and

- L. Yuan, Eds., vol. 10323, Jeju, South Korea, apr 2017, p. 103238F. [Online]. Available: <https://doi.org/10.1117/12.2265632>
- [16] V. Lesnikov, T. Naumovich, A. Chastikov, and D. Garsh, "Unaliasing of undersampled spectra," in *2016 Mediterranean Conference on Embedded Computing*. Institute of Electrical and Electronics Engineers Inc., jul 2016, pp. 124–127. [Online]. Available: <https://doi.org/10.1109/MECO.2016.7525719>
- [17] H. Zainuddin, P. L. Lewin, and P. M. Mitchinson, "Partial discharge characteristics of surface tracking on oil-impregnated pressboard under AC voltages," in *Proceedings of IEEE International Conference on Solid Dielectrics, ICSD*, 2013, pp. 1016–1019.
- [18] P. M. Mitchinson, P. L. Lewin, G. Chen, and P. N. Jarman, "A new approach to the study of surface discharge on the oil-pressboard interface," in *2008 IEEE International Conference on Dielectric Liquids, ICDL 2008*, 2008.
- [19] P. M. Mitchinson, P. L. Lewin, B. D. Strawbridge, and P. Jarman, "Tracking and surface discharge at the oilpressboard interface," *IEEE Electrical Insulation Magazine*, vol. 26, no. 2, pp. 35–41, mar 2010. [Online]. Available: <https://doi.org/10.1109/MEI.2010.5482553>
- [20] G. Hernandez, *Fabry-Perot interferometers*, 1st ed. Cambridge University Press, 1988.